RSC Advances

ROYAL SOCIETY OF CHEMISTRY

www.rsc.org/advances

Journal Name

ARTICLE

IR 820 Stabilized Multifunctional Polycaprolactone Glycol Chitosan Composite Nanoparticles for Cancer Therapy

Received 00th January 20xx,
Accepted 00th January 20xx

DOI: 10.1039/x0xx00000x

www.rsc.org/

Piyush Kumar[a] and Rohit Srivastava[a,*]

Photothermal therapy has gained worldwide attention for its less painful, non invasive/ minimally invasive, effective thermal ablation based therapy for cancer. It has been found effective in the treatment of drug-resistant cancer. Currently available photothermal systems have several limitations such as high cost, incompatibility and clearance from physiological system. To address these issues, we have prepared multifunctional biocompatible and biodegradable cost effective IR 820 dye encapsulated Glycol chitosan coated ploycaprolactone composite nanoparticles (PCLGC-IR) with improved performance. Polycaprolactone (PCL) has been used as a cheap biodegradable polymer while Glycol chitosan (GC) as an immunoadjuvant for immune response generation followed by cost-effective IR 820 dye for photothermal therapy. IR 820 encapsulation increases the stability of PCLGC-IR nanoparticles as confirmed by DSC and XRD, while Glycol chitosan enhances the uptake of composite nanoparticles by MDA-MB-231 breast cancer cells. PCLGC-IR composite nanoparticles of size around 150-200 nm can be irradiated with dual laser 750 nm and 808 nm in photothermal therapy (PTT). In addition to PTT, PCLGC-IR composite nanoparticles can also be used for sustainable control drug release as it retains its structural integrity even after laser treatment. Further we analyzed the degraded product using liquid chromatography mass spectroscopy (LCMS) upon photo irradiation. The cytotoxicity study of PCLGC-IR composite nanoparticles was checked on NIH3T3 cells. Fluorescent microscopic image analysis of MDA-MB-231 cells showed hyperthermic cell death via apoptosis and necrosis due to enhance uptake of PCLGC-IR composite nanoparticles. Our results showed these nanoformulation can be used for effective multiple drug resistant cancer.

Introduction

Photothermal therapy (PTT) has become the buzzword in modern cancer therapy either due to its non-invasive or minimally invasive therapy compared to surgery. PTT uses Near Infra-Red (NIR) absorbing material such as gold, carbon nanotube, graphene oxides or dyes.[12345] These NIR materials upon photo irradiation generate heat. A rise in temperature > 42°C (hyperthermia) has been shown to induce apoptosis in cancer. NIR agents have been extensively used for image-guided effective therapy.[6789] The fluorescent based NIR materials are in great demand for ease in tracking by fluorescent microscope. Photothermal agents like cyanine dyes have inherent fluorescence property. Indocyanine green (ICG), an FDA approved fluorescent cyanine dye has been extensively used as imaging and photothermal agents due to low cytotoxicity. However, poor solubility in water and low stability in the physiological system render its use as effective therapeutic agent.[10] IR 820 has low cytotoxicity and more stability compared to ICG[11]. The fluorescent signal of IR 820 is much stronger than ICG in mouse tail vein after 24 h of injection. Hence, IR 820 has been explored as cost effective imaging agents.[7,12,13,14,15] The heat generation property of IR 820 is nearly same as ICG, makes it suitable for image-guided photothermal therapy. The presence of meso chlorine group in IR 820 facilitated the conjugation of chitosan to IR 820. IR 820-chitosan conjugated showed better cytotoxicity compared to free dye in MES-SA and DX5 cancer cells[16]. Similar study was done with PEG diamine conjugated to IR 820. PEG diamine conjugated showed lower accumulation in kidney and lungs compared to free IR 820 in mice, suggesting the importance of IR 820 nanoformulation in cancer therapeutics.[7]

Although PTT is an effective therapy, to eliminate the reoccurrence of the tumour, chemotherapeutic agents/drugs have also been encapsulated or conjugated with either IR 820 or IR 820 containing formulation.[4,5,17,18] Owing to biodegradable and biocompatible nature, polymeric nanoformulations have been broadly explored. Currently PLGA, an FDA approved polymer has been extensively used for encapsulation of drug and dyes.[4,18,19,20] The amphiphilic nature of this polymer makes it an ideal choice for encapsulation of hydrophobic as well as hydrophilic molecules. However, high cost of PLGA demands cheaper alternative like PCL for novel therapeutic agent. In addition, most of the drugs are hydrophobic in nature, can be easily loaded on PCL.[19] Cost effective and long degradation time makes it an ideal option

[a] *Department of Biosciences and Bioengineering, Indian Institute of Technology-Bombay, Powai, Mumbai-400076, India.*
†*Prof. Rohit Srivastava, Email: rsrivasta@iitb.ac.in Phone No: +9122-25767746.*
Electronic Supplementary Information (ESI) available: [FTIR and UV-VIS data]. See DOI: 10.1039/x0xx00000x

for photo chemotherapy. To improve the efficacy of this polymer, the addition of an immunoadjuvant GC has been proposed for the generation of self-immune response in the cell against cancer. GC, a water-soluble chitosan derivative, has been preferred for encapsulation of drugs at physiological pH. GC has been widely used for the delivery of DNA, anti-cancer agents, and dyes[21,22,23,24,20] GC has also been shown to enhance the fluorescence of the dye to make it better imaging agents.[24] To achieve photothermal effect, we further chose IR 820. IR 820 has been shown to interact with nanoformulation resulting in intrinsic peak shift from 820 to 652 nm in case of chitosan IR conjugate.[16] Several peaks were observed in IR 820 interaction with IRPDcov nanoformulation. The probable explanation for these peak shifts can be attributed to extended л system.[7] The significance of these interactions has not been studied in details. Therefore, the prima facia of the PCLGC-IR nanoformulation is to explore the IR 820 interaction and its significance in optical and surface property for efficient PTT in detail.

In our present study, we have formulated multifunctional PCLGC-IR composite nanoparticles for bioimaging and therapy. According to our knowledge, we explored the significance of IR 820 interaction with PCLGC-IR nanoformulation by DSC, XRD and dual laser (750 nm and 808 nm) for the first time. In addition to that, stability and degradation studies have been checked for the first time by LCMS. Further, the cytotoxicity of PCLGC-IR composite nanoparticles was checked on NIH3T3 cells. Cellular uptake and PTT have been performed on MDA-MB-231 cells. Hence, we explored the multifunctionality of PCLGC-IR composite nanoparticles as bioimaging, PTT, and chemotherapeutic agents.

Experimental

Materials

Polycaprolactone (PCL), poly (vinyl alcohol) Mw: 13,000-23,000, 87-89 % hydrolyzed), glycol chitosan (GC) (MW: 100,000-300,000, degree of polymerization ≥400, Degree of purity ≥75-85%). IR 820 dye, Hoechst 33342, Propidium iodide (PI) were purchased from Sigma-Aldrich. Acetone, dichloromethane, and methanol were purchased from Merck India Pvt. Ltd. DMEM, RPMI 1640, antibiotic-antimycotic solution, Phosphate buffer saline (PBS) with calcium and magnesium salts and trypsin–EDTA solutions were purchased from Himedia Pvt Ltd Mumbai India. All the chemical and reagents used were of analytical grade. MDA-MB-231 cells were purchased from NCCS Pune, India.

Formulation of PCL GCHT IR 820

IR 820 loaded PCL GCHT IR 820 nanoparticles were prepared by oil in water (o/w) emulsion method. Briefly, 10 mg/mL PCL was dissolved in different ratios of DCM-methanol mixture along with 0.3 mg/mL IR 820 dye (ESI). To make the emulsion, the organic phase was slowly added in the aqueous phase containing 0.5 % PVA and 0.1 % GC in water (1:3 ratio). The emulsion was sonicated for 5 min followed by evaporation under magnetic stirring at room temperature. The NPs thus generated were centrifuged at 2500 x g for 15 min to remove large particle and uncoated residues. Finally NPs were collected by centrifuging it 12000 xg for 20 min followed by three washes. To generate uniform separate nanoparticles different ratios of the organic phase DCM: Methanol and Acetone: Methanol and the aqueous phase were also tried.

Characterization of PCLGCHT IR 820

The NPs were characterized by size distribution, poly dispersity and charge by dynamic light scattering and zeta analyzer (Brookhaven Instruments Corporation, USA) respectively. The morphology and size were further analyzed by scanning electron microscope (SEM, JSM 7600F Jeol) and transmission electron microscope (TEM, Jeol 2100F). The absorbance spectra were obtained using UV-visible spectrophotometer (Perkin Elmer lambda 25 USA). The samples were scanned from 400 nm to 1100 nm to determine its absorbance in NIR range. The melting temperature of NPs was determined by DSC. Two mg samples were subjected to scan from 20°C to 100°C with a heating rate of 20°C/min. Fourier transforms infrared spectroscopy (FTIR) is used to determine the chemical structure of nanoparticles. The samples were loaded in KBr pellets. The spectra were recorded by Magna 550 IR spectrophotometer (Nicolet Instrument Corporation). X-Ray Diffraction spectroscopy (XRD) was used to analyze the effect of IR 820 dye encapsulation on composite nanoparticles molecular structure. The powder diffraction patterns were obtained using Philips PW 3040/60 diffractometer with 40 kV, 30 mA graphite filtered Cu KR radiation (λ= 0.1506). Data were scanned from 10° to 80° (2θ) at a scanning speed of 10 degrees per min.

Determination of IR 820 encapsulation:

IR 820 encapsulation was analyzed in triplicate by Uv-Vis spectroscopy. Briefly, a standard curve of IR 820 in DCM and Methanol mixture was plotted.

The lyophilized sample was dissolved in DCM and Methanol mixture. The sample was centrifuged at 15000 rpm for 20 min to remove residual polymeric particles. IR 820 concentration was determined from the standard curved plotted. IR 820 entrapment and loading efficiency was calculated as follow

$$\text{Encapsulation efficiency: } \frac{\text{Amount of IR 820 in NPs}}{\text{Amount of IR 820 used in NPs}} \times 100 \quad \text{.....Eq.1}$$

Stability and degradation studies

The stability of NPs was determined by UV-visible spectrophotometer for 10 days in dark at 4°C. The stability of NPs was also checked in the presence of light and UV for 30 min. The degradation of dye was checked for various parameters such light, UV and temperature for 30 min and with 808 nm (500 mW) laser for 5 min. Degradation of laser treated samples were determined by both UV-visible spectroscopy and Liquid Chromatography-Mass Spectrophotometer (LCMS). The remaining conditions of NPs were also studied by LCMS to determine precise change. NPs stability was also checked using TEM and atomic force microscope (AFM; Asylum research, USA) for any morphological changes.

Photothermal Effect

Photothermal effect of NPs was studied using 750 and 808 nm infrared laser along with digital thermocouple thermometer respectively. Briefly 250 µL (1000 µg/mL) suspensions of NPs were irradiated by either 750 or 808 nm laser for 5min in a 96 well plate inside water bath maintained at 37°C. The rise in temperature was measured at an interval of 1 min.

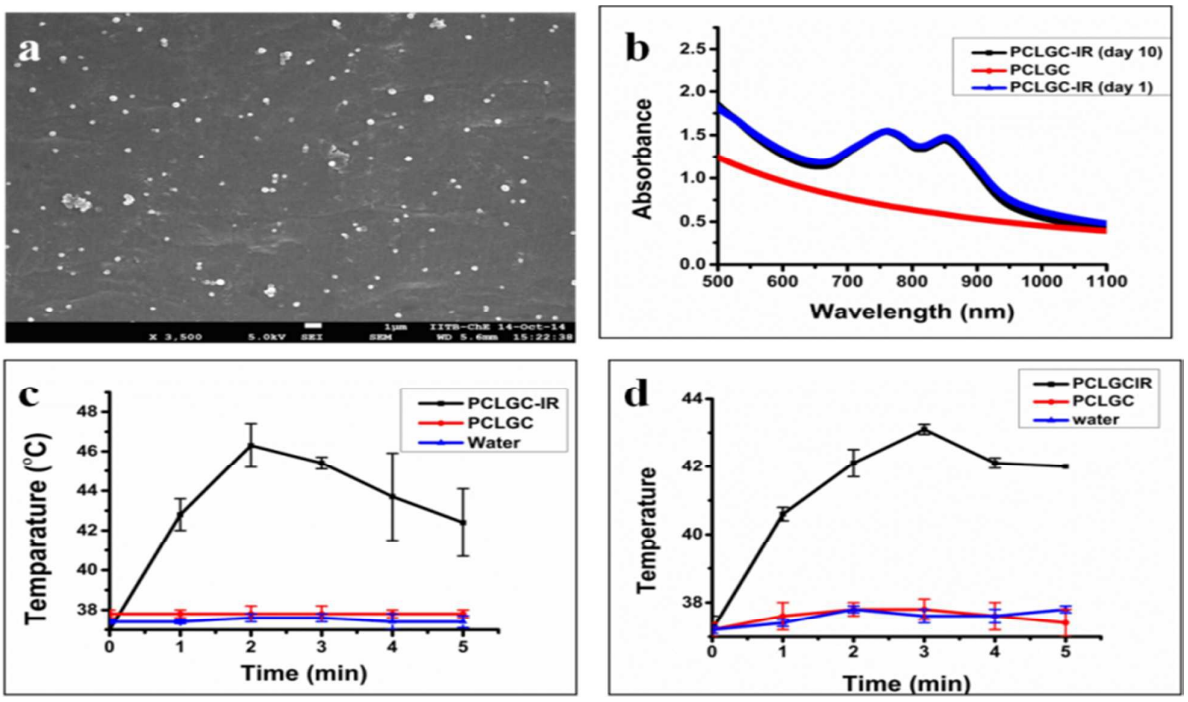

Figure 1 (a) SEM image of PCLGC-IR composite nanoparticles (b) UV-visible absorbance of PCLGC, PCLGC-IR (day 1 and day 10), (c) Photothermal efficiency of PCLGC-IR, PCLGC and water by 808 nm laser (d) Photothermal efficiency of PCLGC-IR, PCLGC and water by 750 nm laser (n=3).

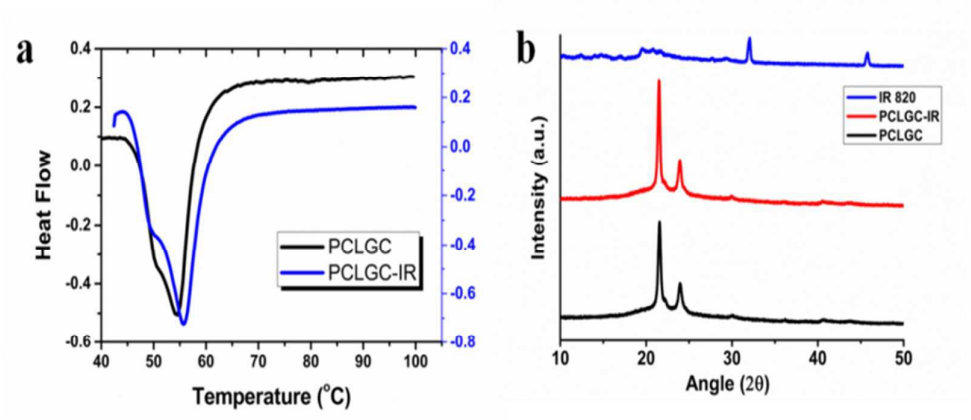

Figure 2 (a) DSC curve of PCLGC and PCLGC-IR nanoparticles (b) XRD data of PCLGC, PCLGC-IR and IR 820.

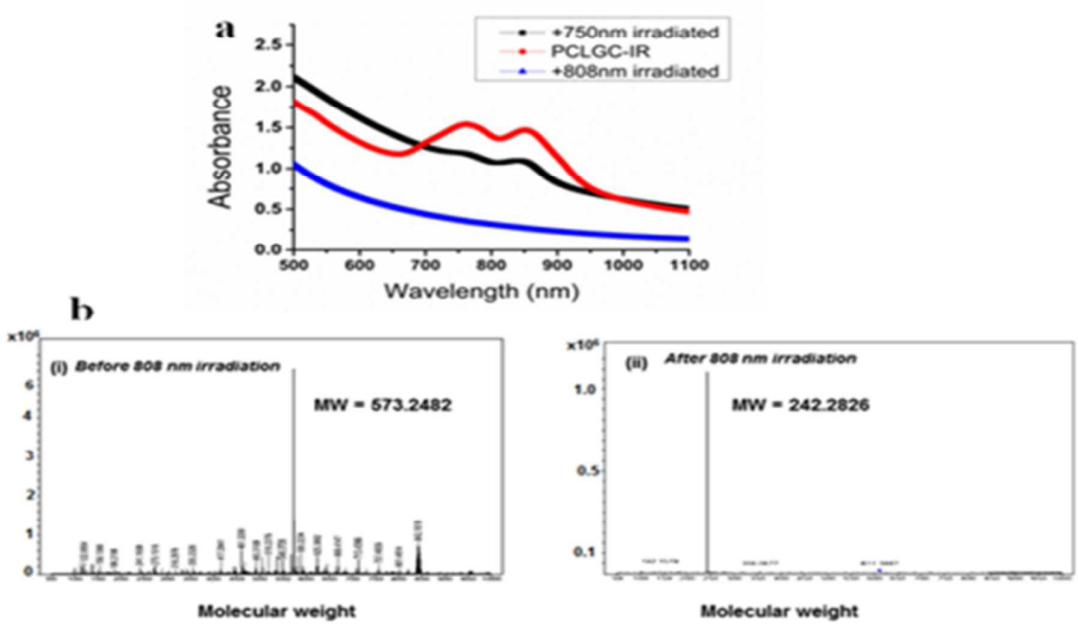

Figure 3 (a) UV-visible absorbance of 808 nm and 750 nm laser treated PCLGC-IR composite nanoparticles (b) i) MS spectra of PCLGC-IR nanoparticles ii) MS spectra of PCLGC-IR nanoparticles after 808 nm laser irradiation.

Cell uptake and *in-vitro* imaging

MDA-MB-231 cells (1 x 10^5) were seeded in 12 well plates under 5 % CO_2 at 37 °C. After 24 h, cells were washed with PBS to remove unattached cells. The cells were incubated with media containing NPs for 4 h. Rhodamine was adsorbed on NPs for visualization under fluorescence microscope. The cells were washed thrice with Phosphate buffer saline (PBS, pH 7.0) to remove any free NPs. Finally PBS with Ca^{2+} and Mg^{2+} was added to the wells for live imaging under Leica microscope (Germany) with λex 528 and λex 551. For quantitative analysis, cells were incubated with free IR 820 dye and PCLGC-IR nanoparticles for 4 h in PBS with Ca^{2+} and Mg^{2+}. At the end of incubation period, supernatant was collected and absorbance was recorded at 820nm in Tecan multiplate reader. The percentage uptake was calculated using formula:

$$\textit{Percentage Uptake} = \frac{[\textit{Total amount of dye used}] - [\textit{Residual dye in supernatant}]}{\textit{Total amount of dye used}} x\ 100$$

$$\ldots . Eq.\ 2$$

Biocompatibility and Photothermal studies on cells

NIH3T3 (1 x 10^4) cells were seeded in 96 well plates and incubated for 24 h under 5 % CO_2 at 37 °C. Medium was replaced with fresh complete media containing NPs (100 µg/mL to 1000 µg/mL). The plate was further incubated for 24 h. Further, the cells were analyzed for viability by MTT assay.

For photothermal effect, MDA-MB-231 (1 x 10^4) cells were seeded into 96 well plate and incubated for 24 h under 5 % CO_2 at 37°C. Medium was replaced with fresh media with 10 % Fetal Bovine Serum (FBS) containing 125 µg/mL of NPs and incubated for 4 h. Cells were washed with PBS and replaced with fresh complete media. Prior laser application, the plate was placed in the dry bath incubator to maintain the temperature of 37°C. Cells were irradiated 808 nm laser (4.2W/cm^2) for 3 min on 4mm spot size. To determine the cytotoxic effect, cells were further subjected to MTT assay.

Apoptosis study by Hoechst PI double staining

For live/ dead, apoptotic and necrotic cells visualization, MDA-MB-231 (1 x 10^5) cells were seeded on a cover slip in 12 well plate under 5 % CO_2 at 37°C. The remaining protocol was similar to photothermal effect as described earlier. At the end of laser application, cells were stained with Hoechst 33342 (10 µg/mL) and incubated at 37°C for 20 min in PBS containing Mg^{2+} and Ca^{2+} ions. Cells were washed with PBS followed by Propidium Iodide (10 µg/mL) staining for 5 min at 37°C. The cells were washed thrice with PBS and visualized under Leica fluorescent microscope (Germany).

Results and discussion

In this study, we have encapsulated IR 820 in PCLGC-IR composite nanoparticles. GC coating on PCL made this composite amphiphilic for successful encapsulation of both hydrophilic and hydrophobic drugs, small chemotherapeutic molecules such as siRNA. We prepared the composite nanoparticles in single oil in water (o/w) emulsion method

using 0.5 % PVA as an emulsifier. Different ratios of DCM and Methanol, Acetone and Methanol were chosen for uniform distribution. Polymers and dye dissolved in 2:1 ratio of DCM and Methanol and 1:3 ratio of organic to aqueous phase showed uniform sphere shaped particles in SEM analysis(ESI).

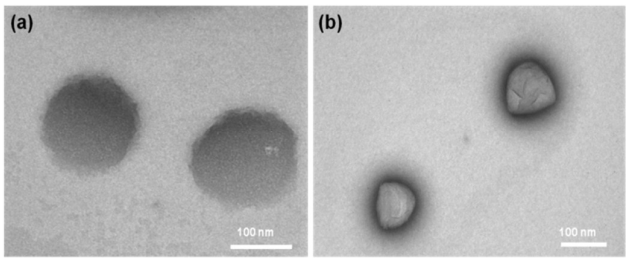

Figure 4: (a) TEM image of PCLGC-IR before laser irradiation (b) TEM image of PCLGC-IR after 808 nm laser irradiation.

240nm with zeta charge around +32 mV ± 3 mV (Table 1). Similar results were observed with ICG encapsulation in PLGA with 3% PVA as an emulsifier.[26] The low amount of PVA in preparation of emulsion results in high loading efficiency of dye in polymer[25]. The encapsulation efficiency of dye was around 48%. PCLGC–IR particles were stable even at low concentration of PVA. UV-visible absorbance (Figure 1b) showed good stability of the dye inside polymer for 10 days at 4°C under dark. The possible reason for stability may be IR 820 interaction with nanoformulation. To explore the interaction of IR 820 dye with nanoformulation, UV-visible, DSC and XRD were performed. UV-visible spectra of PCLGC-IR composite nanoparticles showed two peaks 845 and 750 or 765 nm respectively (Figure 1b). A peak at 845 nm was common in all cases. Whereas, addition peak showed variation depend upon aggregation. A peak at 750 nm was observed for non-aggregated nanoparticles while aggregated nanoparticles

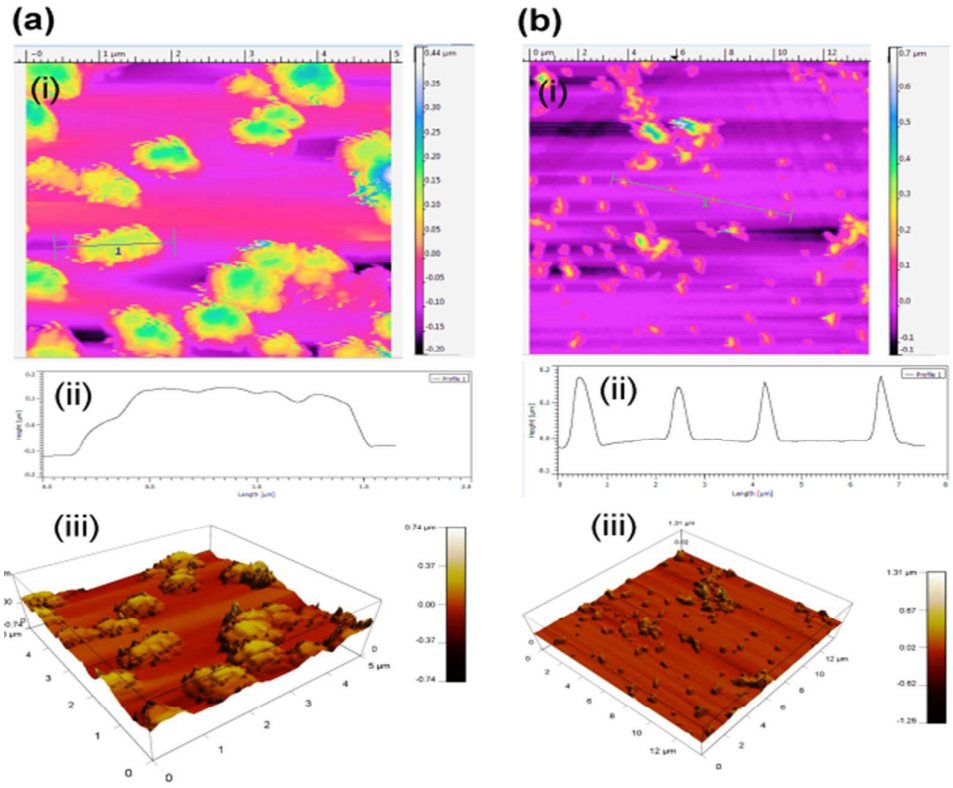

Figure 5: AFM image of PCLGC-IR composite nanoparticles before laser (a) and post laser irradiation (b) after 10 days. The height profile of NPs ((ai) and (bi)) showing an average height of 150-200nm size ((aii) and (bii)) Corresponding 3D images ((aiii)

Table 1 Showing hydrodynamic size and surface charge properties of nanoparticles.

Formulation	Size (nm)	Polydispersity(PDI)	Zeta potential(mV)
PCL NP	120 ± 18	0.194 ± 0.005	-20 ± 4
PCLGC	150 ± 12	0.221 ± 0.04	22 ± 3
PCLGC-IR	240 ± 20	0.158 ± 0.034	32 ± 3

The size distribution of the NPs was around 150-200 nm in SEM (Figure 1a) while the hydrodynamic size was around

showed a peak around 760 nm. The shift in peak from 820 nm to 845 and 750/760 nm may be attributed to extended л system. Peak shift has also been reported in Chitosan IR 820 conjugate.[16]

The interaction of IR 820 with composite nanoformulation was analyzed by FTIR (ESI). The increase in spectral OH hydroxyl group of PCL GC-IR 2930 cm^{-1} and 3440 cm^{-1}, enhanced C=O stretch at 1774 cm^{-1}, enhanced peak at 1180 cm^{-1} was due to addition of sulfonyl group of IR 820 compared to PCL GC

suggested encapsulation of IR 820 in PCL GC. Similar trend was observed in chitosan IR conjugate.[16] This infers that IR 820 interaction with GC is much higher than encapsulation in PCL.

Further stability and interaction of the dye with nanoparticles have been studied by DSC. Blank NPs showed melting temperature around 55°C while dye loaded NPs showed melting temperature around 56°C (Figure 2a). DSC thermogram of dye loaded NPs infers that dye encapsulation increases the stability of particles. Similar thermal studies have been performed in PCL gel polymer to study the effect of interaction of metal with PCL polymer gel[26].

To validate the above results, XRD was performed to know the phase change of PCLGC-IR composite nanoparticles. PCL has

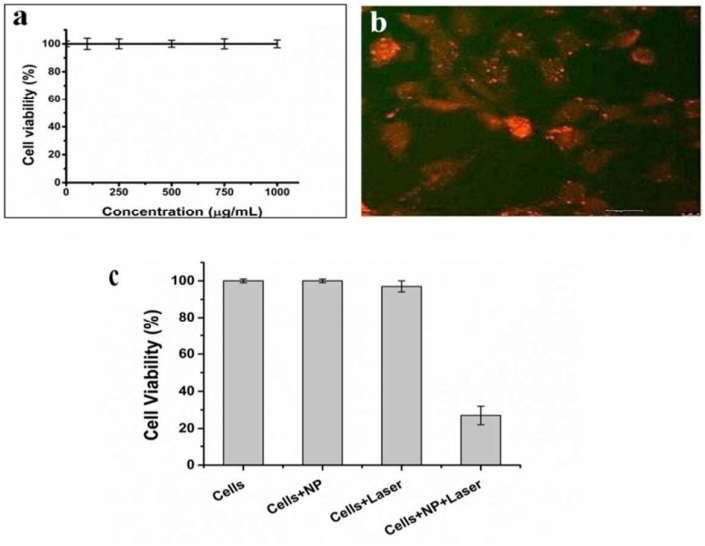

Figure 6: (a) Biocompatibility of PCLGC-IR in NIH3T3 cells, (b) Cellular uptake of Rhodamine labeled PCLGC-IR, and (c) Photothermal therapy of PCLGC-IR with 808 nm laser in MDA-MB-231 cells.

two different characteristic peaks at Bragg's angles 2θ at 21.3° and 23.6° which exhibit orthorhombic unit cell like structure[27]. The addition of GC at low amount did not affect the crystalline structure. However, IR 820 encapsulation in PCLGC-IR increases the intensity of peak of Bragg's angle at 21.6° (Figure 2b). It indicates that addition of either GC or IR 820 did not alter the crystal structure. These data suggest that IR 820 stabilize the crystal structure of PCLGC-IR composite nanoparticles. The interaction of IR 820 is hydrophobic interaction with PCL while hydrophilic with GC. Hence hold the molecules tightly resulting in more crystalline structure. IR 820 incorporation increases the surface charge of PCLGC nanoparticles by +10mV. The MEP analysis of IR 820 dye showed positive to negative charge polarity[28]. So it can interact with both positive and negatively charged molecules. To further validate the interaction of IR 820, spectroscopic analysis was performed for the different concentration of PCL in nanoformulation keeping dye and GC concentration as Constant (ESI).

For photothermal transduction, PCLGC-IR NPs, PCLGC NPs and water were irradiated with 808 nm laser. The maximum temperature rise in PCLGC-IR NPs was 46°C around 1 min followed by drop in temperature suggesting degradation of dye (Figure 1c). The temperature remains above 42 °C till 5 min. Supriya et al has shown that 5μM of IR 820 dye conjugated to chitosan nanoparticles raised the temperature by 6°C using 8W/cm^2 whilst in our case, we have used 4W/cm^2 laser to achieve the same temperature[15].

This might be due to stability of dye inside the NPs as discussed above (Figure 2b). Our results showed an additional absorbance peak around 750-765 nm. Similar shift was also observed with Indocyanine dyes. However, there are no reports on significance of these addition peaks. We also checked the photothermal effect of PCLGC-IR NPs by 750 nm

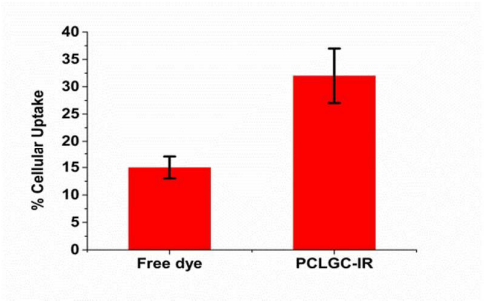

Figure 7. Percentage cellular uptake of free dye and PCLGC-IR in MDA-MB 231 cells.

laser 5W/cm^2 as UV-visible spectra showed an additional peak at 750 nm. The maximum temperature rise was around 43°C after 3 min. The 750 nm laser treatment showed constant temperature rise till 5 min makes it suitable for PTT (Figure 1d). The temperature above 43°C can lead to irreversible cytotoxic effect in cancer. In both cases, blank PCLGC NPs and water did not show any significant increase. This result infers suitability of these NPs for dual laser treatment. In our case, the shift is in the infrared region (750 nm and above) indicating

better efficacy of these NPs for photothermal therapy compared to previously reported articles.[7,15]

To analyze the effect of laser irradiation (750 nm and 808 nm), UV-visible and LCMS analysis have been executed. Interestingly, only one peak was diminished in 750 nm treated sample. While in 808 nm laser treated NPs, both peaks vanished suggesting complete degradation of dye by the laser (Figure 3a).

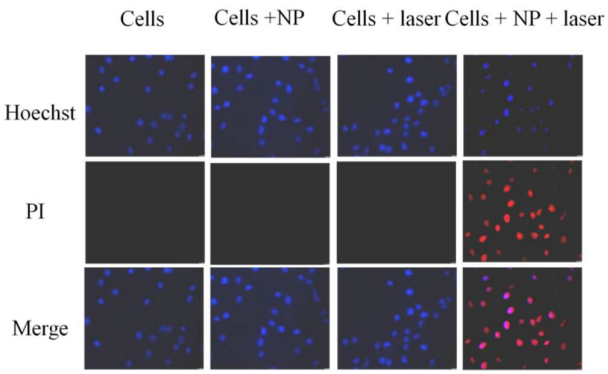

Figure 8: Hoechst PI staining of MDA-MB-231 cells in presence and absence of laser 808 nm laser irradiation and PCLGC-IR.

An 808 nm laser has an advantage of deeper penetration and safety. The fast rise in temperature by 808 nm laser makes it suitable for lower concentration of these PCLGC-IR composite nanoparticles. Hence, the rest of the experiments was performed using 808 nm laser. Cliff yen et al in 2008, have used the MS to detect the degraded product of IR 820 in dog plasma. A peak around 330 Da was reported in the case of degraded IR 820.[29] However, the interaction of IR 820 in any nanoformulation has not been studied. Hence, LCMS studied were performed extensively to predict the effect of laser on IR 820 degradation. To understand the mechanism of degradation, whether it's due to high temperature or photo bleaching, PCLGC-IR composite nanoparticles were subjected to TEM analysis to observe any morphological change and LCMS analysis for degradation studies. To rule out the possibilities of temperature based degradation, PCLGC-IR composite nanoparticles were also subjected to various conditions such light and UV for 30 min and different temperature for 5 min to predict the degradation mechanism.

Table 2: MS spectra of IR 820 dye in different condition inside the composite nanoparticles.

Sr. No.	Experimental conditions	MS spectra (Da)	Change in Spectra (Da)
1.	25°C for 30 min	573	Nil
2.	37°C for 30 min	573	Nil
3.	Light for 30 min	573	Nil
4.	Near UV for 30 min	573	Nil
5.	UV for 30 min	573	Nil
6.	808 nm laser irradiation for 5 min	242	331
7.	40°C for 5 min	573	Nil
8.	45°C	573	Nil
9.	47°C	573	Nil

All the samples showed a major peak around 573 Dalton (Da) except 808 nm laser treated samples. In case of 808 nm laser, the sample showed a peak around 242 Da (Table 1). It is difficult to analyze the dye inside body once it degrades as it loses its fluorescence ability. The peak at 573 Da and 242 Da can be used to trace the dye inside the physiological system by Mass spectroscopy before and after the laser irradiation (Figure 4b). The peak at 573 Da may refer to heterocyclic nitrogen ring that imparts fluorescence and 808 nm absorbing compound. This also infers that the compound of molecular weight around 573 Da is responsible for the photothermal effect. It indicates the laser-based degradation of the dye due to photo bleaching. As different temperature ranging from 37°C to 47°C for 5 min did not show any change.

However, longer incubation at higher temperature degrades the dye. TEM analysis showed no morphological changes in freshly prepared untreated and laser treated particle, suggesting these particles can also be used for controlled drug delivery (Figure 4). A further study is going on to evaluate the significance of these degraded products and its significance in conjugation chemistry. We confirmed the effect of laser irradiation on PCLGC-IR NPs after 10 days at room temperature under dark condition by AFM (Figure 5). AFM analysis revealed PCLGC-IR composite nanoparticles before laser irradiation gets aggregated due to release of IR 820 dyes (fig 5a), while no change was observed in laser irradiated PCLGC-IR nanoparticles as laser degraded the IR 820 dye (Figure 5b). PCLGC-IR composite nanoparticles remained morphologically intact after 12 days. The size distribution remained same around 150-200 nm. This further validates our hypothesis for controlled release of therapeutics (drugs/ nucleic acid) using PCLGC-IR composite nanoparticles even after PTT.

IR 820 has lower cytotoxicity compared to ICG and IR78 dyes.[13] However, free IR 820 above 10 µmol has been shown toxic to the cells[15]. The cytotoxicity of PCLGC-IR composite nanoparticles was tested on NIH3T3 mouse fibroblast cells. Our results showed PCLGC-IR nanoparticles are non-toxic compared to free IR 820 (Figure 6a). This suggests its suitability for *in vivo* studies. Further, the cellular localization of Rhodamine labeled NPs was studied using the confocal microscope (Figure 6b). The enhanced cellular uptake can be attributed to the interaction between positively charged glycol chitosan coating and negatively charged cancer cell surface. The cellular uptake PCLGC-IR nanoparticles were 2 times higher than that of free dye at the end of 4h (Figure 7).

In vitro photothermal effect was analyzed on MDA-MB-231 cells (Figure 6c). MDA-MB 231 is a triple negative breast cancer cell line. It is sensitive to hyperthermia. Since most of the triple Negative breast cancer cells are getting drug resistant; hence, we chose these cells lines to check the effectiveness of our NPs onto them. Laser irradiated PCLGC-IR composite nanoparticles showed 3 fold reductions in cell viability in comparison to control cells. The significant hyperthermic cell death was observed due to high cellular uptake of the positively charged PCLGC composite nanoparticles. To visualize cell death, Hoechst 33342 and PI double stain were done (Figure 8). The controls did not show any PI stained cells inferring that bare

PCLGC NPs or Laser alone did not cause immediate cell death. However cells treated PCLGC-IR NPs and laser showed both apoptotic (deeply stained by Hoechst) and necrotic cells (stained with PI) indicating the possible mechanism of cell death by both apoptosis and necrosis. The cytotoxicity of PCLGC-IR composite nanoparticles can be further improved by combining chemotherapy. Thus, PCLGC-IR composite nanoparticles can be effectively used for cancer theranostic.

Conclusions

We successfully formulated biocompatible and biodegradable PCLGC-IR composite nanoparticles for effective cancer theranostic. IR 820 composite nanoparticles can be used for image-guided photothermal therapy. PCL and GC add benefit for encapsulation of a chemotherapeutic molecule such drug along with dye. IR 820 dye encapsulation enhanced the stability of composite nanoparticles as observed by DSC. The stability of these NPs in aqueous solution makes them suitable for in vivo applications. Hence, we speculate that PCLGC-IR composite nanoparticles can also be used for photothermal chemotherapy. GC also enhances the cellular uptake of these composite nanoparticles that lead to significant hyperthermic cell death in MDA-MB-231 cells. IR 820 has been shown to give more than one peaks upon encapsulation. In our case, two peaks were observed. For the first time, we studied the photothermal effect of the addition peak. These composite nanoparticles can be used with dual laser system 750 nm and 808 nm laser diode for photo irradiation. We further studied the stability and degradation of the IR 820 dye in composite nanoparticles by LCMS. The LCMS study can further help in analyzing the clearance of the dye through the physiological system. In summary, these composite nanoparticles can be used for multimodal cancer theranostic. The further detail studies of the PCLGC-IR composite nanoparticles are on the way understand its true potential as a cancer theranostic agent.

Acknowledgements

The authors would like to acknowledge SAIF-IITB and chemical engineering department for characterization studies. We are thankful to Rohit Teotia, Rajan Singh and Narendra Jha for their help during the experiment. We are also thankful to Manish Kumar for their help in writing manuscript. P.K. is thankful to Indian Council of Medical Research, New Delhi for senior research fellowship [(File no. 3/1/3/JRF-2008/HRD-102(32238)]. The authors also acknowledge IITB-Healthcare for financial support.

Note: All experimental data have been represented as mean± S.D.(P< 0.05) with n=3.

References

1 A. K. Rengan, A. B. Bukhari, A. Pradhan, R. Malhotra, R. Banerjee, R. Srivastava and A. De, 2015.
2 W. Miao, G. Shim, S. Lee and Y. K. Oh, *Biomaterials*, 2014, **35**, 4058–4065.
3 S. Z. Nergiz, N. Gandra, S. Tadepalli and S. Singamaneni, 2014.
4 M. Zheng, C. Yue, Y. Ma, P. Gong, P. Zhao, C. Zheng, Z. Sheng, P. Zhang, Z. Wang and L. Cai, *ACS Nano*, 2013, **7**, 2056–67.
5 P. Xue, K. K. Y. Cheong, Y. Wu and Y. Kang, *Colloids Surfaces B Biointerfaces*, 2015, **125**, 277–283.
6 M. Zheng, P. Zhao, Z. Luo, P. Gong, C. Zheng, P. Zhang, C. Yue, D. Gao, Y. Ma and L. Cai, *ACS Appl. Mater. Interfaces*, 2014, **6**, 6709–6716.
7 A. Fernandez-, R. Manchanda and T. Lei, 2014, 4631–4648.
8 W. Guo, L. Zhang, J. Ji, W. Gao, J. Liu and M. Tong, *Tumour Biol.*, 2013.
9 L. Wu, S. Fang, S. Shi, J. Deng, B. Liu and L. Cai, *Biomacromolecules*, 2013, **14**, 3027–3033.
10 A. Fernandez-Fernandez, R. Manchanda, T. Lei, D. a. Carvajal, Y. Tang, S. Z. R. Kazmi and A. J. McGoron, *Mol. Imaging*, 2012, **11**, 99–113.
11 D. S. Conceição, D. P. Ferreira and L. F. V. Ferreira, *Int. J. Mol. Sci.*, 2013, **14**, 18557–71.
12 A. Manuscript, *Changes*, 2012, **29**, 997–1003.
13 F. N. I. R. Fluorescent, J. L. Lakshmi, S. Bin Dolmanan and S. Tripathy, 2013, 6796–6805.
14 P. Huang, P. Rong, A. Jin, X. Yan, M. G. Zhang, J. Lin, H. Hu, Z. Wang, X. Yue, W. Li, G. Niu, W. Zeng, W. Wang, K. Zhou and X. Chen, 2014, 6401–6408.
15 S. Srinivasan, R. Manchanda, A. Fernandez-Fernandez, T. Lei and A. J. McGoron, *J. Photochem. Photobiol. B Biol.*, 2013, **119**, 52–59.
16 Y. Yuan, Z. Wang, P. Cai, J. Liu, L.-D. Liao, M. Hong, X. Chen, N. Thakor and B. Liu, *Nanoscale*, 2015, **7**, 3067–3076.
17 S. Su, Y. Tian, Y. Li, Y. Ding, T. Ji, M. Wu, Y. Wu and G. Nie, ACS Nano, 2015, **24**, 1367-78.
18 P. Zhao, M. Zheng, C. Yue, Z. Luo, P. Gong, G. Gao, Z. Sheng, C. Zheng and L. Cai, *Biomaterials*, 2014, **35**, 6037–6046.
19 A. Kumari, S. K. Yadav and S. C. Yadav, *Colloids Surfaces B Biointerfaces*, 2010, **75**, 1–18.
20 S. Srinivasan, R. Manchanda, T. Lei, A. Nagesetti, A. Fernandez-Fernandez and A. J. McGoron, *J. Photochem. Photobiol. B Biol.*, 2014, **136**, 81–90.
21 H. Koo, K. H. Min, S. C. Lee, J. H. Park, K. Park, S. Y. Jeong, K. Choi, I. C. Kwon and K. Kim, *J. Control. Release*, 2013, **172**, 823–831.
22 S. Kim, D. J. Lee, D. S. Kwag, U. Y. Lee, Y. S. Youn and E. S. Lee, *Carbohydr. Polym.*, 2014, **101**, 692–698.
23 J. Rhee, O. K. Park, A. Lee, D. H. Yang and K. Park, 2014, 6038–6057.
24 S. Lee, S. W. Kang, J. H. Ryu, J. H. Na, D. E. Lee, S. J. Han, C. M. Kang, Y. S. Choe, K. C. Lee, J. F. Leary, K. Choi, K. H. Lee and K. Kim, *Bioconjug. Chem.*, 2014, **25**, 601–610.
25 A. P. Ranjan, K. Zeglam, A. Mukerjee, S. Thamake and J. K. Vishwanatha, *Nanotechnology*, 2011, **22**, 295104.
26 C. P. Fonseca, F. C. Jr, F. a Amaral, C. a Z. Souza and S. Neves, *Int. J. Electrochem Sci.*, 2007, **2**, 52 – 63.

27 M. Borjigin, C. Eskridge, R. Niamat, B. Strouse, P. Bialk and E. B. Kmiec, *Int. J. Nanomedicine*, 2013, **8**, 855–864.
28 T. B. V Neves and G. F. S. Andrade, 2015, **2015**.
29 C. Y. Chen, R. M. Fancher, Q. Ruan, P. Marathe, A. D. Rodrigues and Z. Yang, *J. Pharm. Biomed. Anal.*, 2008, **47**, 351–359.